Absorption Spectra Analysis of a Laboratory Photoionised Plasma

I. M. Hall, T. Turmaz, and R. C. Mancini
University of Nevada, Reno

J. E. Bailey and G. Rochau
Sandia National Laboratories

M. Rosenberg and D. Cohen
Swarthmore College

I. Golovkin and J. MacFarlane
Prism Computational Sciences

M. Sherril and J. Abdallah
Los Alamos National Laboratory

R. Heeter, M. Foord, and S. Glenzer
Lawrence Livermore National Laboratory
(Dated: December 14, 2008)

The Z facility at the Sandia National Laboratories is the most powerful terrestrial source of X-rays and provides an opportunity to produce photoionised plasmas in a relatively well characterised radiation environment. We use a detailed atomic-kinetic and spectral simulations to analyse absorption spectra of photoionised neon driven by the x-ray flux from a z-pinch. The broadband x-ray flux both photoionises and backlights the plasma. In particular, we focus on estimating the charge state distribution of the plasma and the characteristics of the ionising radiation field in order to estimate the ionisation parameter.

PACS numbers:

I. INTRODUCTION

Photoionised plasmas are common in astrophysical environments, typically occurring near strong sources of X-rays such as active galactic nuclei and X-ray binaries. In recent years, the Chandra and XMM-Newton satellites have recorded high resolution spectra from astrophysical photoionised plasmas. These spectra contain a wealth of spectroscopic information and have motivated new efforts aimed at obtaining a detailed understanding of the atomic-kinetic and radiative characteristics of photoionised plasmas. However, models used to interpret spectra from astrophysical plasmas are complex and have many parameters including the geometry of the system, gas composition, density distribution and energy distribution of the driving X-ray flux. Uncertainties inherent in these parameters will affect the validity of the results obtained from the spectral analysis.

In photoionised plasmas, the radiation field plays a dominant role in the atomic-kinetic behaviour, and collisional processes do not strongly influence the ionisation balance. In contrast, the ionisation balance in most laboratory plasmas is largely determined by collisional processes. The requisite conditions of strong radiation field and low collisionality are difficult to achieve experimentally, and there have been relatively few studies of terrestrial photoionised plasmas. The Z facility at Sandia National Laboratories is currently the most powerful terrestrial source of X-rays, and is capable of producing a photoionised plasma[1]. Indeed, wire-array Z-pinch experiments at Z can yield 1–2MJ of X-ray energy with a peak power of up to 200TW in a short pulse of ∼6ns duration.

In this paper, we present the analysis of data from an experiment at Sandia in which X-rays from a collapsing Z-pinch plasma were used to photoionise low density neon contained in a gascell. The analysis method allows the charge state distribution of the photoionised plasma to be estimated by fitting spectral absorption features across several ionisation stages. This 'proof of principle' experiment provides the starting point for a further series of experiments currently in progress. The aim of these experiments is to produce a photoionised plasma with a simple geometry, known ion number density and quantified X-ray heating flux. Spectra from the well characterised plasma will provide a dataset which can be used to test the accuracy of atomic data and simulation codes. The photoionised nature of the plasma makes this data relevant to photoionised plasmas in astrophysics.

The paper is organised as follows. In section II we discuss details of the charge state analysis method and apply the method to the absorption spectra of a photionised neon plasma to infer the charge state and interpret the observed spectral features. In section III we use the inferred charge state distribution along with atomic-kinetic simulations to estimate the characteristics of the driving

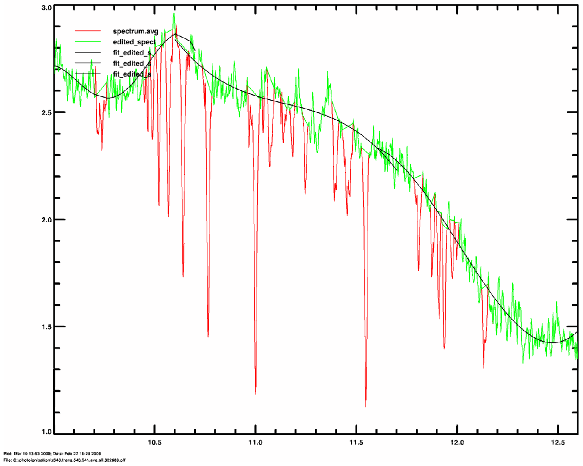

FIG. 1: Example of fitting background to averaged transmission data.

X-ray flux heating the neon plasma. These values allow us to estimate a value for the ionisation parameter of the plasma.

II. ANALYSIS

Details of the experimental setup can be found in ref. [1]. In brief, the broad band Z-pinch radiation drives the gascell, photoionising the neon gas and also acting as a backlighter for absorption measurements. Time integrated spectra were recorded using two space-resolving convex KAP crystal spectrometer. Each instrument records two spectra on each shot, providing a total of up to four spectra. Post processing of the raw data to obtain transmission spectra comprised several stages[2]. A total of seven spectra were sucessfully obtained from two shots with nominally identical gascell and Z-pinch parameters. These data were averaged together to improve the signal to noise ratio, and to help discriminate between real spectral features and possible crystal defects. The background continuum of the averaged spectra was fitted using several low order polynomial curves covering different wavelength regions. Figure 1 shows a small region of the averaged experimental data with polynomials fitted to three of the spectral regions. Spectral lines were edited out to separate out absorption features from the background continuum. The background used during the fitting procedure is shown by the green portion of the curve, whilst the spectral absorption lines are shown in red. Fitting the background in this way was necessary as no independent measure of the unattenuated Z-pinch spectrum was made. The transmission spectra was then found by dividing fitted continuum by the averaged data.

The analysis method is based on absorption spectra measurements and provides similar information to the 'curve of growth' method commonly used in the astrophysical community to estimate the charge state distribution from observed absorption spectra. The method we use to infer the charge state distribution is based on computing synthetic transmission spectra for a given set of ion densities in the H, He and Li charge states. These are compared to experimental spectra to determine the set of 'best fit ion' densities. The total ion density, charge state distribution and mean ion charge then follow as a result.

Photon energy resolved opacities in each ion stage are required to compute synthetic transmission spectra. We use the PrismSpect code[3], to generate energy resolved opacities in the H, He and Li-like ionisation stages over a range of ion number densities between 10^{16} and 10^{18}cm^{-3}. A detailed level collisional-radiative atomic model was used. Configuration averaging was used for ion stages from neutral to Be-like. Term splitting and fine structure were used for the energy levels in the Li-like to H-like charge states. In particular, the Li-like ion stage included doubly excited states $1s2lnl'$ with $n \leq 8$. This setup gives us an accurate population balance across all ionisation stages and a high level of detail from the charge states of spectroscopic interest, namely the H, He and Li-like stages.

In the simulation, the incident X-ray radiation field was specified by a diluted Planckian with brightness temperature of 40eV and colour temperature of 200eV. The electron and ion temperature were held fixed at $T_e = T_i = 25$eV. These values correspond to estimates of the plasma and radiation environment in the centre of the gascell at the peak of the Z-pinch emission, provided by simulations of the radiation environment at the gascell and the hydrodynamic behaviour of the neon. We note that for these plasma conditions, the majority of the population in each ion stage is in the ground state and so line absorption transitions occur mostly from the ground state.

The radiation environment at the gascell was modelled using the Visrad view factor code[4]. From a user specified geometry and radiation source the code computes the radiation environment at a given position, taking into account the re-radiated emission from different parts of the setup. The hydrodynamics of the gascell were simulated using the Helios code[5], using the radiation field at the gascell from the Visrad simulation as the driving X-ray flux. This provides estimates of the temperature and density evolution of the gascell in response to the radiation field. More detailed discussion of the Visrad and Helios simulations can be found ref [6].

Uniform plasma conditions were assumed over a distance of 14mm, corresponding to the line of sight through the gascell including the bowing effect of the mylar windows due to the gas pressure. Computed spectra were convolved with a Gaussian lineshape to account for the spectral resolution of the instrument of $\lambda/\Delta\lambda \sim 900$. Energy resolved transmission (T_ν) is then computed from the sum of the energy resolved opacities in each ion stage from

$$T_\nu = \exp(-\tau_\nu L) \tag{1}$$

$$\tau_\nu = \sum_i \sigma_{\nu,i}\rho_i \tag{2}$$

. τ_ν is the total optical depth (cm^{-1}), $\sigma_{\nu,i}$ is the opacity (cm^{2}g^{-1}) of ion stage i and ρ_i its mass density (g cm^{-3}). The plasma is assumed to be uniform with a length L=1.4cm.

In order to extract the ion charge distribution from the absorption spectra, a genetic algorithm (GA) was used to search the set of ion stage densities that provide the best match with the experimental spectra[7][8]. A population of 200 was used, and each population member was given 4 genes to represent the densities in the H, He, Li and Be-like ion stages. The genes are initialised to random values. The 'fitness' of a particular set of ion densities is based on the χ^2 value between the synthetic with measured spectra calculated using

$$\chi^2 = \sum_\nu \frac{(T_\nu^{\rm Exp} - T_\nu)^2}{T_\nu} \tag{3}$$

, where $T_\nu^{\rm Exp}$ is the experimental transmission at frequency ν and T_ν the transmission for the ion density combination at the same frequency. ν runs over the entire frequency range being fitted. The 'fitness' for the ion density combination is then given by $1/\chi^2$. The fittest sets of ion densities emerge after several generations of evolution using single point crossover and mutation, giving the set of ion densities that best fit the experimental spectra. 100 generations were used for the fitting procedure and generally the best solution was reached by generation 50. By selecting the ion density for each charge state independently, we are able to construct a transmission spectra for a plasma with arbitrary charge state distribution.

The GA method allows us to determine the 'best fit' ion densities in a robust fashion, starting from an unbiased initial guess. Repeating the search using different seed values for the random number generator was found to have negligible impact on the final solution. In addition to the charge state distribution, the GA also provides an estimate of the total ion density from the sum of the density in each ion stage. Comparison with the nominal fill pressure of the gascell provides a consistency check to help evaluate the validity and accuracy of the analysis.

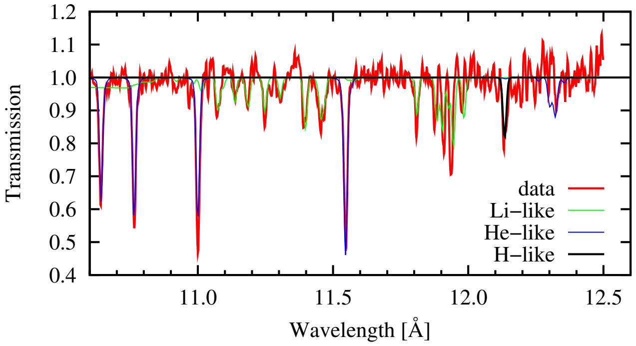

FIG. 2: Fit obtained to experimental spectra.

Figure 2 shows the averaged experimental spectra overlaid with the best fit result from the model. The fitted result gives a total ion density of 1.060×10^{18}cm^{-3} with ion fractions H-like=0.007, He-like=0.899, Li-like=0.0.094, and a mean ion charge of 7.91. The total ion density compares favourable with the nominal fill pressure used in the experiment of $\sim 10^{18}$ cm^{-3}. Contributions to the spectrum from the different ion stages are shown by the green, blue and black curves, corresponding to Li, He and H-like charge states respectively. The Lyα line (in black) is at ∼12.1Å, whilst the He-like resonance line series (1snp → 1s^2) lie at shorter wavelengths, from n=3 at 11.55Å to n=11 at ∼ 10.45Å. The series of Li-like satellites to Heγ (11–11.5Å) and Heβ (11.5–12Å) observed experimentally are well resolved by the model, in terms of both the relative strength and wavelengths of the lines.

The agreement with measured spectra is good overall and we have a reasonable agreement with the observed relative strengths of the features from the H to Li-likes ion stages. The wavelengths of the observed features are well reproduced. Particularly noteworthy is the presence of the Li-like satellites (green curve) from $1s2lnl' - 1s^22l$ transitions. Satellites to the Heβ line ($n = 3$) lie between 11.7 and 12.0Å, whilst satellite to Heγ, δ and higher order lines ($n \geq 4$) lie between 11 and 11.5Å. Experimental spectra show evidence of satellites up to around $n = 6, 7$ close to the Heγ line at 11Å.

III. IONISATION PARAMETER

The inferred charge state distribution and ion density can be used to estimate the colour and brightness temperature characteristic of the ionising flux of radiation in the experiment. From this, we may then calculate the ionisation parameter of the plasma, defined by[9]

$$\xi = 4\pi I/{\rm N_e} \quad ({\rm erg\ cm\ s^{-1}}) \tag{4}$$

, where I is the ionising flux of radiation (erg cm^{-2} s^{-1}) and N_e the electron number density (cm^{-3}). I is related to the brightness temperature, T_B, by the Stefan-Boltzmann law $I = \sigma T_B^4$. The ionisation parameter is a measure the relative importance of the collisional and photoionisation processes in the plasma and is a commonly used quantity in astrophysical applications. The regime of astrophysical interest is ξ ∼1–1000 erg cm s^{-1}.

A further series of PrismSpect simulations was carried out, with the objective of identifying the radiation field and electron temperature most consistent with the charge state distribution estimate in Part II. The radiation field was assumed to be Planckian, characterised by

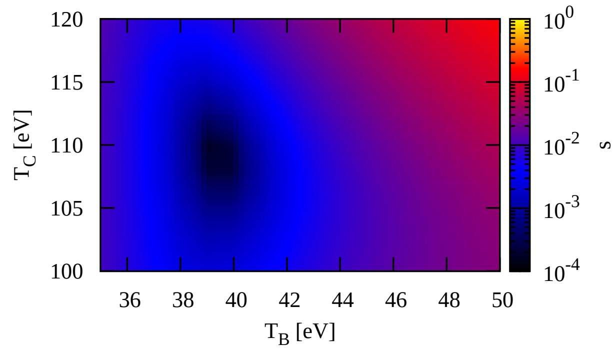

FIG. 3: s as a function of T_C and T_B for an electron temperature of 30eV.

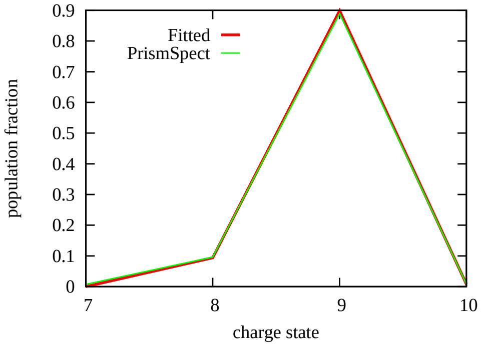

FIG. 4: Charge state population fractions from the optimum PrismSpect simulation (T_C=110eV, T_B=39eV, T_e=30eV) overlaid with the distribution inferred from the absorption spectra.

a colour and brightness temperature (T_C and T_B respectively) with values T_B=10...60eV with 5eV increments and T_C=80...240eV with 10eV increments. The ion density was uniform and held fixed at 10^{18}cm^{-3}. The charge state distribution for each T_C, T_B combination was compared with the values inferred from the experimental spectra and the sum of squares between the two distributions calculated using

$$s = \sum_i \left(\frac{f_i^{\text{fitted}} - f_i^{\text{PrismSpect}}}{f_i^{\text{fitted}}} \right)^2 \tag{5}$$

, where f_i is the fractional population in ion stage i and i runs over all the fitted charge states (i.e. H to Li-like). Values of T_C and T_B that give the smallest value of s provide an estimate for the radiation field in the neon plasma consistent with the inferred charge state. Several scans of T_C and T_B were carried out using electron temperatures ranging from 25 to 35eV. In this way we were able to determine values of T_C, T_B and T_e that give an overall minimum value of s and therefore estimates of plasma and radiation conditions most consistent with the fitted charge state and observed spectra.

We found that T_e=30eV with T_B=39eV and T_C=110eV gave the smallest value of s, with a mean ion charge of 7.90. Figure 3 shows the variation of s in the region of $T_C - T_B$ space close to the best solution, illustrating that there is a reasonably well defined minimum region in parameter space. From the optimum brightness temperature, we estimate the ionisation parameter, ξ to be approximately 3.78 erg cm s^{-1}. If we assume that the uncertainty in the value of T_B is ±1eV, then we have an error in ξ of $\Delta\xi \sim 0.3$. Figure 4 shows the charge state distribution from the PrismSpect simulation overlaid with the values inferred from the absorption spectra in Part II. We have a good agreement in the population fractions across all charge states fitted to the experimental spectra.

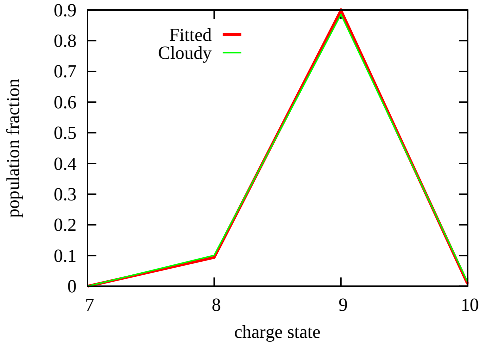

FIG. 5: Charge state population fractions from the optimum Cloudy simulation (T_C=105eV, T_B=44eV, T_e=55eV) overlaid with values inferred from the absorption spectra.

An important part of this work is to make the connection between the laboratory photoionised plasma and the astrophysical situation. To this end, we also used the astrophysical simulation code Cloudy[10] to infer the ionisation parameter, employing the same method as with the PrismSpect code. Cloudy was configured to compute the electron temperature and ionisation balance in a 1.4cm layer of neon plasma self consistently with an external radiation field. As in the PrismSpect simulation, the radiation was Planckian and characterised by the colour and brightness temperature. The simulation was set up to search for T_C and T_B values giving the best match to ion charge state densities inferred from experimental spectra. A grid of T_C, T_B values were also computed, to confirm the existence of a well defined region of optimum solution in parameter space.

The best fit was obtained for the parameters T_B=44eV, T_C=105eV with an average electron temperature of T_e=55eV and mean ion charge of 7.90. Again, as shown in fig. 5, we obtain good agreement with the ion fractions inferred from the experimental data. This value of T_B gives an ionisation parameter of ξ=6.11 erg cm s^{-1}.

In general we have a reasonable agreement between the radiation field parameters inferred by fitting the charge state distribution with PrismSpect and Cloudy.

IV. DISCUSSION AND CONCLUSIONS

In this paper we have presented a method that can be used to infer charge state distribution from an absorption spectra of a photoionised plasma. It was found possible to produce a good match to the experimental spectra across all three ion stages, giving a measure of the Li to H-like charge state ion densities and assisting identification of absorption features.

We then searched for sets of colour and brightness temperatures that give the best match to the inferred charge state distribution in order to infer the ionisation parameter of the plasma. It was found possible to produce a good fit to the inferred charge state distribution using a uniform neon plasma driven by a diluted Planckian X-ray flux, characterised by a colour and brightness temperature and electron temperature.

We note that the T_C values from PrismSpect and Cloudy are quite similar at 110 and 105eV respectively, and that both are significantly lower than the estimates colour temperature used in Part II of 200eV. The 200eV value is the characteristic colour temperature of the Z-pinch itself, however the flux reaching the neon is affected by absorption from the front mylar wall of the gascell. The true neon driving flux is therefore not Planckian and there is significant absorption due to oxygen and carbon absorbers at energies between 200 and 600eV. The 105-110eV colour temperatures obtained here could be providing an approximation of the true drive flux in order to produce a similar effect on that charge state distribution of the neon.

The PrismSpect and Cloudy brightness temperatures (39eV and 44eV respectively) are reasonably close to each other, but correspond to a difference of ∼60% in absolute x-ray flux driving the neon. The electron temperature for the Cloudy solution of 55eV is significantly higher than the best fit value from PrismSpect of 30eV. The temperature calculation in Cloudy will investigated further in future work to attempt to understand these differences. It is likely that additional radiative losses could be partially responsible. This would also impact the T_B value obtained when fitting to the inferred ion densities.

One important addition to this work is the inclusion of errors associated with the experimental data and inferred ion stage densities. This would help to estimate a range of possible ionisation parameters using PrismSpect and Cloudy and decide whether differences between results from each code are significant.

[1] J. E. Bailey et al. Neon photoionization experiments driven by z-pinch radiation. *Journal of Quantitative Spectroscopy and Radiative Transfer*, 71:157–168, 2001.

[2] J. E. Bailey. Private communication, 2008.

[3] J. J. MacFarlane et al. Simulation of the ionization dynamics of alumunium irradiated by intense short-pulse lasers. *Proceedings of Inertial Fusion and Science Applications*, 2003.

[4] J. J. MacFarlane. VISRAD - a 3-d viewfactor code and design tool for high-energy density physics experiments. *Journal of Quantitative Spectroscopy and Radiative Transfer*, 81:287–300, 2003.

[5] J. J. MacFarlane and I. E. Golovkin and P. R. Woodruff. HELIOS-CR a 1-d radiation-magnetohydrodynamics code with inline atomic kinetics modeling. *Journal of Quantitative Spectroscopy and Radiative Transfer*, 99:381–397, 2006.

[6] I. M. Hall et al. Modelling, design and diagnistics for a photoionised plasma experiment. *Astrophysics and Space Science*, DOI - 10.1007/s10509-008-9930-4, 2008.

[7] David E. Goldberg. *Genetic Algorithms in Search, Optimization, and Machine Learning.* Addison-Wesley, 1989.

[8] I. E. Golovkin et al. Analysis of x-ray spectral data with genetic algorithms. *Journal of Quantitative Spectroscopy and Radiative Transfer*, 75:625–636, 2002.

[9] B. Remington and R. P. Drake and D. D. Ryutov. Experimental astrophysics with high power lasers and z pinches. *Reviews of Modern Physics*, 78:755–807, 2006.

[10] G. J. Ferland et al. CLOUDY 90: Numerical simulation of plasmas and their spectra. *Publications of the Astronomical Society of the Pacific*, 110:761–778, 1998.